



## Real-time observation of the dry oxidation of the Si(100) surface with ambient pressure x-ray photoelectron spectroscopy

Yoshiharu Enta, Bongjin S. Mun, Massimiliano Rossi, Philip N. Ross Jr., Zahid Hussain, Charles S. Fadley, Ki-Suk Lee, and Sang-Koog Kim

Citation: *Applied Physics Letters* **92**, 012110 (2008); doi: 10.1063/1.2830332

View online: <http://dx.doi.org/10.1063/1.2830332>

View Table of Contents: <http://scitation.aip.org/content/aip/journal/apl/92/1?ver=pdfcov>

Published by the [AIP Publishing](#)

---

### Articles you may be interested in

[Initial oxidation of Si\(110\) as studied by real-time synchrotron-radiation x-ray photoemission spectroscopy](#)  
*J. Vac. Sci. Technol. B* **27**, 547 (2009); 10.1116/1.3021032

[In situ observation of wet oxidation kinetics on Si\(100\) via ambient pressure x-ray photoemission spectroscopy](#)  
*J. Appl. Phys.* **103**, 044104 (2008); 10.1063/1.2832430

[Stability of cerium oxide on silicon studied by x-ray photoelectron spectroscopy](#)  
*J. Vac. Sci. Technol. B* **19**, 1611 (2001); 10.1116/1.1387464

[Atomic-level study of the robustness of the Si\(100\)-2×1:H surface following exposure to ambient conditions](#)  
*Appl. Phys. Lett.* **78**, 886 (2001); 10.1063/1.1348322

[X-ray photoelectron spectroscopy investigations of the chemistries of soils](#)  
*J. Vac. Sci. Technol. A* **17**, 1079 (1999); 10.1116/1.581778

---

A horizontal banner with an orange-to-yellow gradient background. The text '2014 Special Topics' is centered in a large, white, sans-serif font. Below the text are five circular icons, each containing a different material structure and a label: 'PEROVSKITES' (red and black lattice), '2D MATERIALS' (blue and red lattice), 'MESOPOROUS MATERIALS' (green and blue porous structure), 'BIOMATERIALS/ BIOELECTRONICS' (yellow and black structure), and 'METAL-ORGANIC FRAMEWORK MATERIALS' (brown and yellow porous structure). At the bottom left is the 'AIP | APL Materials' logo. At the bottom right is a red ribbon with the text 'Submit Today!' in white.

2014 Special Topics

PEROVSKITES

2D MATERIALS

MESOPOROUS MATERIALS

BIOMATERIALS/ BIOELECTRONICS

METAL-ORGANIC FRAMEWORK MATERIALS

AIP | APL Materials

Submit Today!

## Real-time observation of the dry oxidation of the Si(100) surface with ambient pressure x-ray photoelectron spectroscopy

Yoshiharu Enta<sup>a),b)</sup>

Faculty of Science and Technology, Hirosaki University, 3 Bunkyo-cho, Hirosaki 036-8561, Japan

Bongjin S. Mun<sup>a),c)</sup>

Department of Applied Physics, Hanyang University, Ansan, Kyeonggi 426-791, Korea, and Advanced Light Source, Lawrence Berkeley National Laboratory, Berkeley, California 94720, USA

Massimiliano Rossi, Philip N. Ross, Jr., and Zahid Hussain

Advanced Light Source, Lawrence Berkeley National Laboratory, Berkeley, California 94720, USA

Charles S. Fadley

Department of Physics, University of California-Davis, Davis, California 95616, USA, and Material Sciences Division, Lawrence Berkeley National Laboratory, Berkeley, California 94720, USA

Ki-Suk Lee and Sang-Koog Kim

Research Center for Spin Dynamics &amp; Spin-Wave Devices and Nanospintronics Laboratory, Department of Materials Science and Engineering, College of Engineering, Seoul National University, Seoul 151-744, Republic of Korea

(Received 20 September 2007; accepted 10 December 2007; published online 3 January 2008)

We have applied ambient-pressure x-ray photoelectron spectroscopy with Si 2*p* chemical shifts to study the real-time dry oxidation of Si(100), using pressures in the range of 0.01–1 Torr and temperatures of 300–530 °C, and examining the oxide thickness range from 0 to ~25 Å. The oxidation rate is initially very high (with rates of up to ~225 Å/h) and then, after a certain initial thickness of the oxide in the range of 6–22 Å is formed, decreases to a slow state (with rates of ~1.5–4.0 Å/h). Neither the rapid nor the slow regime is explained by the standard Deal-Grove model for Si oxidation. © 2008 American Institute of Physics. [DOI: 10.1063/1.2830332]

Silicon dioxide and other dielectric layer thicknesses in the range of a couple tens of angstroms or less are now of critical importance in the semiconductor industry. However, there is very little data concerning the oxidation process in this regime, with the available results being either for layers thicker than this grown under high pressure conditions<sup>1–3</sup> or for only the first couple of monolayers as studied under high vacuum conditions. For example, Massoud *et al.*<sup>3</sup> have reported data for the oxidation rate between about 20 and 500 Å in detail, but there is little or no experimental data extending continuously from 20 Å downward. Accurate experimental data in this range are thus needed in order to better understand and exploit this oxidation regime. It is also known that the often-used Deal-Grove (DG) model for silicon oxidation may not be applicable for oxide thicknesses less than about 250 Å.<sup>3</sup>

In this study, the oxidation rate of a Si(100) surface for oxide thicknesses from 0 up to ~25 Å was measured using chemical-state-resolved ambient-pressure x-ray photoelectron spectroscopy (APXPS). For comparison, ellipsometry is a commonly used method for measuring oxide thickness, but it is difficult to obtain oxide thicknesses below 20 Å with high accuracy. By contrast, in APXPS, we can monitor the Si 2*p* core levels during oxidation, with the spectra having high sensitivity to the surface and chemically-shifted components, as shown in the inset of Fig. 1, finally permitting a determination of the oxide thickness with what has been estimated is

1–2 Å precision.<sup>4</sup> In addition, APXPS spectra can be taken in real time, as detailed below.

Such real-time APXPS measurements *in situ* can avoid several experimental errors in comparison to *ex situ* procedures in which the surface is oxidized in one chamber, then pumped to high vacuum, and finally transferred to the XPS chamber for analysis. However, prior XPS studies of Si oxidation in real time have been limited by the fact that the measurements generally require high vacuum environments

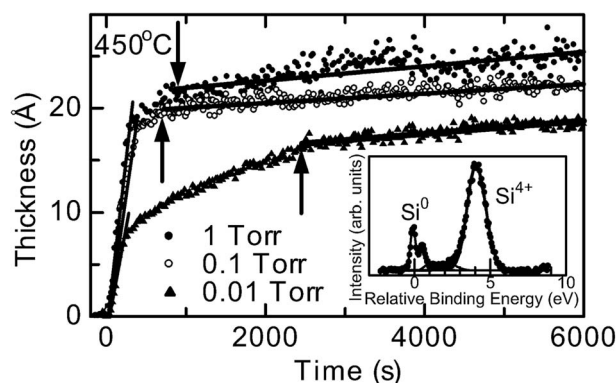


FIG. 1. Main panel: Time evolution of the oxide thickness measured at an oxidation temperature of 450 °C and at oxygen pressures of 1 Torr (closed circles), 0.1 Torr (open circles), and 0.01 Torr (triangles). The oxygen gas was introduced into a reaction chamber at time=0. The arrows indicate the approximate points of transition between the rapid and slow regimes. Solid lines show least square fits of the data in the rapid and slow regimes. Inset: a typical Si 2*p* core-level spectrum recorded at 350 eV photon energy from an ~22-Å-thick oxide on Si(100) grown at the substrate temperature of 450 °C (dots) as well as a best fit by a least-square fitting procedure using spin-orbit split Voigt functions (solid curves).

<sup>a)</sup> Authors to whom correspondence should be addressed.

<sup>b)</sup> Electronic mail: enta@cc.hirosaki-u.ac.jp.

<sup>c)</sup> Electronic mail: bsmun@lbl.gov.

in the sample region; thus, the oxygen pressures have been limited to  $10^{-5}$  Torr or less.<sup>5,6</sup> In this pressure regime, the oxidation reaction almost stops at an oxide thickness of 4–6 Å, which corresponds to 1 or 2 ML of oxide.<sup>7–9</sup> Therefore, oxidation at higher ambient oxygen pressures is necessary to form the thicker oxide. Recently, our group and its collaborators have developed a high-pressure XPS system, which, by means of a windowed synchrotron radiation beam for excitation and differential pumping between the sample region and the energy analysis region, can operate at ambient gas pressures up to  $\sim 5$  Torr.<sup>10</sup>

The silicon substrate was cut from a mirror-polished, B-doped Si(100) wafer, chemically cleaned using the RCA method,<sup>11</sup> and then annealed by resistive heating at 1000 °C in ultrahigh vacuum in the APXPS chamber. The cleanliness of the surface was verified by Si 2*p* core-level spectra, which showed no evidence of oxide peaks (cf. inset in Fig. 1 from an oxidized surface). The photon energy was set at 350 eV, as derived from Beamline 9.3.2 at the Berkeley Advanced Light Source. The radiation was incident at 15° with respect to the surface, and the photoelectrons were emitted normal to the surface.

The Si 2*p* core-level spectrum of oxidized Si exhibits a bulk-silicon component ( $\text{Si}^0$ ) and various oxide components that are up to about 4.4 eV higher binding energy (cf. inset of Fig. 1).<sup>12</sup> Although there is still some disagreement as to the origin of each component, as well as suggestions of the existence of additional components,<sup>13–16</sup> the main peak located at around 0.0 eV relative binding energy is accepted as that of elemental Si ( $\text{Si}^0$ ) and that at 4.4 eV as that of the stoichiometric oxide ( $\text{Si}^{4+}$ ). From the measured ratio of  $\text{Si}^{4+}$  intensity to  $\text{Si}^0$  intensity and previous analyses of experimental data<sup>4,12,16</sup> that yield the electron inelastic mean free path in the oxide at our energy as 9.8 Å and the ratio of intensities from pure bulk Si and pure bulk  $\text{SiO}_2$  as 1.47, the thickness of stoichiometric oxide can be calculated.<sup>4,12</sup> For example, the  $\text{SiO}_2$  thickness in the inset of Fig. 1 is estimated at 21.5 Å.

Each Si 2*p* spectrum was accumulated for 30 s and this process was continued for 2 h under several oxidation conditions. In order to obtain good signal/noise ratios with this accumulation time, we reduced the energy resolution of the photoemission spectrometer in comparison with the spectrum in Fig. 1, but resolving the two peaks of interest ( $\text{Si}^0$  and  $\text{Si}^{4+}$ ) was nonetheless easily possible.

Figure 1 shows the time evolution of the 4+ oxide thickness measured at an oxidation temperature of 450 °C and at three different pressures of 0.01, 0.1, and 1.0 Torr. The curves show that the oxidation starts with a very rapid rate just after the oxygen pressure is quickly raised to each value, and that an oxide layer of  $\sim 10$ – $20$  Å very quickly forms, with the curves for 1 and 0.1 Torr being very similar. Oxidation at 0.01 Torr is not surprisingly slower, but all three curves exhibit a thickness regime above 17–22 Å in which the rate is much slower, and the thickness achieves something approximating a saturation value. We will, thus, use the terms “rapid regime” and “slow regime” to distinguish these two kinds of behavior. While the rate in the rapid regime depends somewhat on the oxygen pressure, that is to say is smaller at lower pressure, the thickness of the break point dividing the rapid regime and the slow regime is constant at  $\sim 16$ – $22$  Å among the three curves. However, at the lowest pressure of 0.01 Torr, the slow regime starts at a somewhat

TABLE I. Oxidation rates in the rapid (slow) regimes derived from the results in Figs. 1 and 2 (underlined values) and other data not shown here.

	300 °C	400 °C	450 °C	530 °C
0.01 Torr		68(3.9) Å/h	143(2.2) Å/h	216(2.8) Å/h
0.1 Torr		137(1.5) Å/h	179(1.5) Å/h	
1 Torr	64(2.1) Å/h	173(1.8) Å/h	234(2.5) Å/h	

lower oxide thickness of about 17 Å and there is an approach to it from 8 to 17 Å that is of intermediate slopes. We have fit linear curves to the data in both the rapid and slow regimes and the oxidation rates so derived are given in Table I.

Figure 2 shows the time evolution of the oxide thickness measured at an oxygen pressure of 1 Torr and three different temperatures of 300, 400, and 450 °C. The behavior of the rate curves is basically similar to those in Fig. 1; that is, they are characterized by a rapid regime and a slow regime. However, the oxide thickness at the break point dividing the regimes strongly depends on the oxidation temperature. The thickness becomes larger as the temperature is increased,  $\sim 6$  Å at 300 °C,  $\sim 18$  Å at 400 °C, and  $\sim 22$  Å at 450 °C.

Although the DG model is not used to describe kinetics in the thickness regime below about 250 Å, it is in any case interesting to check whether at least our slow regime might correspond to the linear (or interface-kinetics-limited) regime of the linear-then-parabolic growth expected in this model. The results in Table I in parentheses represent the experimental rates. Looking at the variation of these rates with pressure, we see that the data at 0.01 Torr show on average larger oxidation rates in the slow regime in comparison with those at 0.1 and 1 Torr. This could be due to the fact that the saturation oxide thickness at 0.01 Torr is somewhat lower than that at 0.1 and 1 Torr, and that there is, thus, less of a diffusion barrier to oxidation from an overall kinetics point of view, a mixing of the two effects included in the DG model. The rates for 1 Torr are on average higher than for 0.1 Torr, which can be reasoned simply on the basis of increased pressure with the same onset saturation thickness. Within the statistical accuracy of our linear fits, we do not see a distinct monotonic relationship between the slow-regime growth rates and either the oxidation temperature or the oxidation pressure. Again comparing to the DG model, we note that the linear rate constant has a large activation

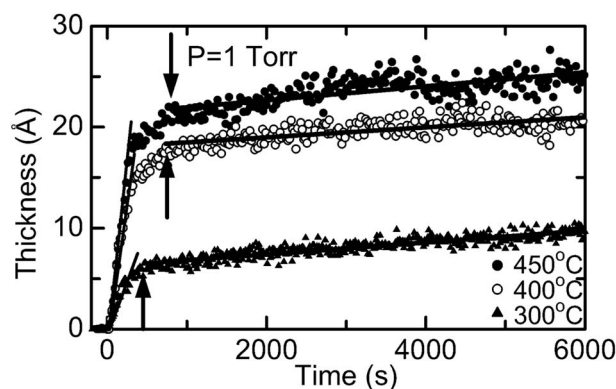


FIG. 2. Time evolution of the oxide thickness measured at an oxygen pressure of 1 Torr and at the temperatures of 450 °C (closed circles), 400 °C (open circles), and 300 °C (triangles). The arrows indicate the approximate points of transition between the rapid and slow regimes. Solid lines show least square fits of the data in the rapid and slow regimes.

energy of  $\sim 2.0$  eV, and that the rate should also be proportional to the oxygen pressure,<sup>1,17</sup> with neither of these aspects being present in the experimental data. Moreover, all the oxidation rates in Table I in the slow regime are larger than  $1 \text{ \AA/h}$ , whereas the linear rate constant based on the DG model can be estimated to be less than  $3 \times 10^{-4} \text{ \AA/h}$  at 1 Torr and  $600 \text{ }^\circ\text{C}$ , somewhat beyond our temperature range.<sup>1</sup> The rates we obtained at temperatures between  $300$  and  $530 \text{ }^\circ\text{C}$  are, thus, considerably larger than those deduced by the DG model, and those in the rapid regime (again see Table I), which are between  $64$  and  $234 \text{ \AA/h}$  for our conditions of temperature and pressure, are even further away from the predictions of this model. As another comparison to prior work, the initial rates in a previous study of Si(100) oxidation that began at  $\sim 7\text{--}15 \text{ \AA}$  of native oxide (about where our slow regime begins) and used a much higher dry oxygen pressure of  $7.6$  Torr (as diluted by argon) and temperature ( $800 \text{ }^\circ\text{C}$ ) were  $\sim 48 \text{ \AA/h}$ .<sup>3</sup> This rate can be scaled to  $1.0$  Torr from this prior data,<sup>3</sup> which indicates a dependence on oxygen pressure as  $(\text{pressure})^{0.8}$ , to yield  $\sim 9.6 \text{ \AA/h}$ , which is considerably larger than those in our slow regime, but at a higher temperature at which this qualitative difference would be expected. So there is thus no fundamental disagreement with these prior experiments.

As a final aspect of our data, the temperature dependence of our data at a given pressure in the rapid regime has been analyzed to yield an approximate value for the effective activation energy, and this yields numbers between  $0.2$  and  $0.4$  eV. These values are considerably lower than those found previously for somewhat thicker oxides on Si(100), which are about  $2.4$  eV.<sup>3</sup>

In summary, the dry oxidation of clean Si(100) up to  $\sim 25 \text{ \AA}$  has been investigated by real-time APXPS. The oxidation rate is found to show two regimes: a rapid regime just at the beginning of oxidation and a subsequent slow regime in which the growth is much reduced. The oxide thickness of the break point dividing the two regimes is between about  $6$  and  $22 \text{ \AA}$  and strongly depends on the oxidation temperature as well as the pressure. Our data cannot be explained by the DG model, but the rate curves presented here should provide a unique test of alternative kinetic models in this important parameter regime. For example, Monte Carlo approaches<sup>18,19</sup> have been proposed for modeling Si oxidation dynamics and a comparison between our data and rates calculated using this type of theoretical modeling would be interesting for the

future. The further application of APXPS to problems of interest in semiconductor technology as, e.g., the growth of high- $k$  dielectric layers, is most promising. In this direction, we are planning future studies with a higher luminosity spectrometer and better multichannel detection that should permit resolving all oxidation states as a function of time.

This work was supported by the U.S. Department of Energy under Contract No. DE-AC03-76SF00098. C.S.F. was supported by the Humboldt Foundation, the Helmholtz Association, the Jülich Research Center, and the University of Hamburg. Y.E. was supported by Overseas Advanced Education and Research Program from the Ministry of Education, Culture, Sports, Science, and Technology of Japan. K.S.L. and S.K.K. were supported by Creative Research Initiatives (ReC-SDSW) of MOST/KOSEF.

<sup>1</sup>B. E. Deal and A. S. Grove, *J. Appl. Phys.* **36**, 3770 (1965).

<sup>2</sup>C. Krzeminski, G. Larrieu, J. Penaud, E. Lampin, and E. Dubois, *J. Appl. Phys.* **101**, 064908 (2007), and references therein.

<sup>3</sup>H. Z. Massoud, J. D. Plummer, and E. A. Irene, *J. Electrochem. Soc.* **132**, 2685 (1985); **132**, 2693 (1985).

<sup>4</sup>M. P. Seah and S. J. Spencer, *Surf. Interface Anal.* **33**, 640 (2002).

<sup>5</sup>H. Horie, Y. Takakuwa, and N. Miyamoto, *Jpn. J. Appl. Phys., Part 1* **33**, 4684 (1994).

<sup>6</sup>Y. Enta, Y. Miyanishi, H. Irimachi, M. Niwano, M. Suemitsu, N. Miyamoto, E. Shigemasa, and H. Kato, *Phys. Rev. B* **57**, 6294 (1998).

<sup>7</sup>Y. Enta, Y. Miyanishi, H. Irimachi, M. Niwano, M. Suemitsu, N. Miyamoto, E. Shigemasa, and H. Kato, *J. Vac. Sci. Technol. A* **16**, 1716 (1998).

<sup>8</sup>A. Yoshigoe, K. Moritani, and Y. Teraoka, *Jpn. J. Appl. Phys., Part 1* **42**, 3976 (2003).

<sup>9</sup>S. Ogawa and Y. Takakuwa, *Jpn. J. Appl. Phys., Part 1* **45**, 7064 (2006).

<sup>10</sup>D. F. Ogletree, H. Bluhm, G. Lebedev, C. S. Fadley, Z. Hussain, and M. Salmeron, *Rev. Sci. Instrum.* **73**, 3872 (2002).

<sup>11</sup>W. Kern and D. A. Puotinen, *RCA Rev.* **31**, 187 (1970).

<sup>12</sup>F. J. Himpsel, F. R. McFreely, A. Taleb-Ibrahimi, J. A. Yarmoff, and G. Hollinger, *Phys. Rev. B* **38**, 6084 (1988).

<sup>13</sup>M. M. Banaszak Holl and F. R. McFreely, *Phys. Rev. Lett.* **71**, 2441 (1993).

<sup>14</sup>F. Jolly, F. Rochet, G. Dufour, C. Grupp, and A. Taleb-Ibrahimi, *J. Non-Cryst. Solids* **280**, 150 (2001).

<sup>15</sup>J. H. Oh, H. W. Yeom, Y. Hagimoto, K. Ono, M. Oshima, N. Hirashita, M. Nywa, A. Toriumi, and A. Kakizaki, *Phys. Rev. B* **63**, 205310 (2001).

<sup>16</sup>S. Dreiner, M. Schürmann, and C. Westphal, *Phys. Rev. Lett.* **93**, 126101 (2004).

<sup>17</sup>R. M. C. de Almeida, S. Gonçalves, I. J. Baumvol, and F. C. Stedile, *Phys. Rev. B* **61**, 12992 (2000).

<sup>18</sup>Y. Tu and J. Tersoff, *Phys. Rev. Lett.* **89**, 086102 (2002).

<sup>19</sup>K. Tatsumura, T. Watanabe, D. Yamasaki, T. Shimura, M. Umeno, and I. Ohdomari, *Jpn. J. Appl. Phys., Part 1* **43**, 492 (2004).